

EFFECTS OF HEAT-FLOW AND HYDROTHERMAL FLUIDS FROM VOLCANIC INTRUSIONS ON AUTHIGENIC MINERALIZATION IN SANDSTONE FORMATIONS

Wolela Ahmed*

Department of Petroleum Operations, Ministry of Mines, P.O. Box 486, Addis Ababa, Ethiopia

(Received December 8, 2000; revised April 26, 2002)

ABSTRACT. Volcanic intrusions and hydrothermal activity have modified the diagenetic minerals. In the Ulster Basin, UK, most of the authigenic mineralization in the Permo-Triassic sandstones pre-dated tertiary volcanic intrusions. The hydrothermal fluids and heat-flow from the volcanic intrusions did not affect quartz and feldspar overgrowths. However, clay mineral-transformation, illite-smectite to illite and chlorite was documented near the volcanic intrusions. Abundant actinolite, illite, chlorite, albite and laumontite cementation of the sand grains were also documented near the volcanic intrusions. The abundance of these cementing minerals decreases away from the volcanic intrusions.

In the Hartford Basin, USA, the emplacement of the volcanic intrusions took place simultaneous with sedimentation. The heat-flow from the volcanic intrusions and hydrothermal activity related to the volcanics modified the texture of authigenic minerals. Microcrystalline mosaic albite and quartz developed rather than overgrowths and crystals near the intrusions. Chlorite clumps and masses were also documented with microcrystalline mosaic albite and quartz. These features are localized near the basaltic intrusions. Laumontite is also documented near the volcanic intrusions. The reservoir characteristics of the studied sandstone formations are highly affected by the volcanic and hydrothermal fluids in the Hartford and the Ulster Basin. The porosity dropped from 27.4 to zero percent and permeability from 1350 mD to 1 mD.

KEY WORDS: Heat-flow, Hydrothermal fluids, Volcanic intrusion, Authigenic mineralization, Ulster Basin, Hartford Basin

INTRODUCTION

The regional geology of Northern Ireland has been summarized by [1, 2]. Various workers [3-5] have discussed the sub-surface geology of the Ulster Basin. The Post-Permian basin history of the Ulster Basin has been summarized in [1, 6]. Several workers [7-9] have investigated the petroleum potential of Northern Ireland basins. The sedimentology, diagenesis and reservoir potential of the Permo-Triassic sandstones has been studied by Ahmed [10].

The depositional environments of the Hartford Basin are well documented in [11-14]. Basin development and major episodes of rift-basin formation and filling are well documented in [13, 15-19]. Several workers [10, 14, 20, 21] have investigated the diagenesis of different sandstone formations in the Hartford Basin. This paper accounts the effects of heat-flow and hydrothermal fluids from volcanic intrusions on authigenic mineralization in sandstone formations in the Ulster and Hartford Basins.

The major factors which control diagenesis of sandstone and other clastic sediments include: temperature, pore water chemistry, fluid flow, mineralogical partitioning, depositional environment, tectonic setting, time, depth of burial and time of uplift, geothermal gradient and subsurface pressure [22-24, 10]. Therefore, reconstruction of the diagenetic history of minerals at different part of the sandstone body is vital in understanding porosity and permeability to predict the reservoir characteristics of sandstones. Chemical reaction between rock forming

*Corresponding author. E-mail: Wolela_am@yahoo.com

minerals and any fluids that are injected into the reservoir, and stability fields of minerals with respect to the pore water are vital in understanding of diagenetic processes [25]. Hydrothermal fluids and heat-flow from the volcanic intrusions that are injected into the sandstone depositional environments have impact on mineral formation and mineral transformation.

Understanding of mineralization processes is vital in sandstone diagenesis and reservoir characteristics studies. The types of minerals formed during sandstone diagenesis have direct effects on reservoir characteristics. Studies were conducted on 1-2 meter thick volcanic dikes and sills to understand heat-flow and hydrothermal fluids effects on minerals formation, and transformation and their impact on reservoir characteristics. The Permo-Triassic sandstones of the Ulster Basin, UK and the Triassic-Jurassic sandstones of the Hartford Basin, USA, were considered for case studies. The Triassic-Jurassic sandstones in the Hartford Basin were deposited contemporaneously with volcanic activities, whereas the Permo-Triassic sandstones of the Ulster Basin were intruded later by Tertiary volcanics.

Microcrystalline mosaic albite and quartz, actinolite, chlorite, illite and laumontite near the intrusions have modified the reservoir characteristics. Illite reduces permeability considerably by blocking the pore throat. Secondary porosity is reduced by shard-like (sheaves) of actinolite. Pore-bridging smectite and chlorite have the worst effect in destroying the porosity and permeability. Albite and laumontite also reduced pore spaces. The studied sandstone formations attain maximum porosity and permeability up to 27.4% and 1350 mD, respectively. However, near the intrusions the porosity value drops to zero and permeability less than 1 mD. Therefore, large volcanic intrusions within the sandstone bodies need attention in oil exploration.

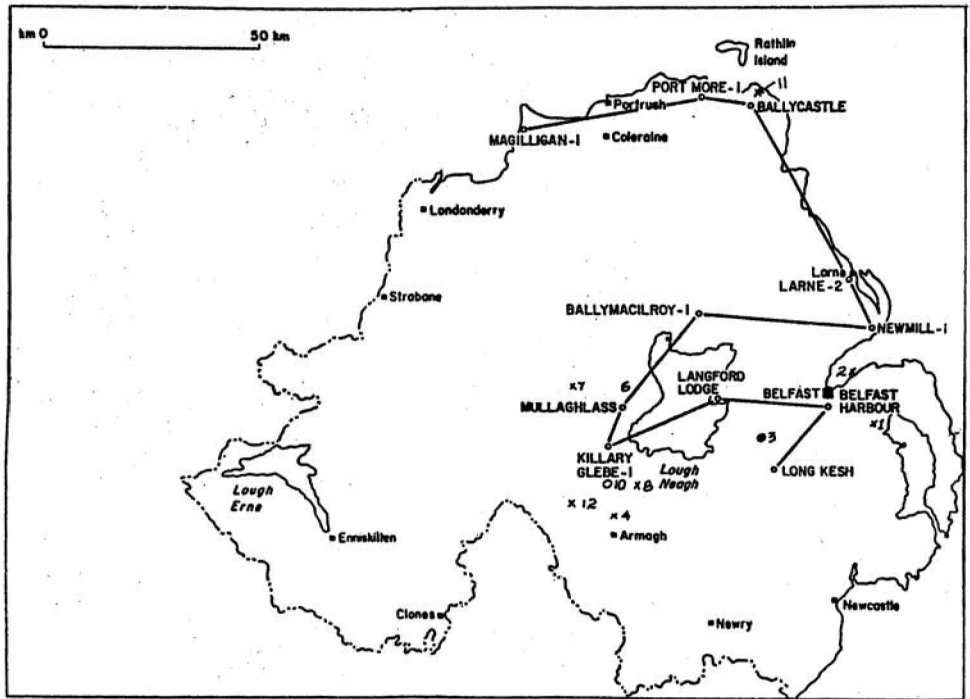


Figure 1. Location map of studied area in the Ulster Basin (1 = Scrabo, 2 = Cultra, 3 = borehole 4B, 4 = Dorlies, 5 = Draperfield, 6 = Coalisland, 7 = Templerreagh borehole, 8 = Twyford Mill, 9 = Ballyloughan Bridge, 10 = Elm Bush, 11 = Murlough Bay, 12 = Mill Town, 13 = Prince of Wales Bridge, 14 = Red Ford).

EXPERIMENTAL

Sections were logged and samples were collected near the intrusions and away from the intrusions. The studied areas are shown in Figure 1 and 5. All of the sandstone samples were impregnated with blue resin (blue-dyed araldite) for petrographic study to highlight porosity. Resin-impregnated thin sections were examined using a transmitted light microscope, and their modal composition evaluated by point counting 500 points per thin section [26].

Gold-coated chip samples were examined under a JEOL 6400 scanning electron microscope equipped with energy dispersive X-ray analysis (EDX) system with accelerating voltage of 10 to 15 kV, to study the morphology, mineral composition, distribution and paragenesis of the authigenic minerals and pore throat geometry. Quantitative analyses were carried out using a JEOL 733 super probe with an accelerating voltage of 15 kV, probe current of 1×10^{-8} A and spot size $1 \mu\text{m}$ [27]. Carbon-coated polished chips and thin sections were used for probe analyses to identify mineral composition, mineral transformation and zoning in cementing minerals and the textural relationships of the authigenic minerals [28].

RESULTS AND DISCUSSION

Background geology of the Ulster Basin

The Permo-Triassic sandstones of the Ulster Basin had been accumulated in rapidly subsiding fault-bounded onshore basins, as has been elsewhere in the British Isles. The Permo-Triassic sandstones lie on the Dalradian, the Carboniferous and the Old Red Sandstone, and are capped by the Mercia Mudstone Group [1, 2]. The Ulster Basin is a rift-related extensional sedimentary basin. The development of the basin has passed through three major orogenies (Caledonian, Variscan and Alpine) [29]. The NE-SW trending fault-bounded asymmetrical graben was infilled with 10,000 meters thick rudaceous, arenaceous, argillaceous, carbonate and evaporite deposits. The general chrono-lithostratigraphy and tectonic phases of the Ulster Basin are shown in Figure 2. The basin underwent multiple phases of uplift and erosion in the Upper Jurassic and Mid-Cretaceous, and also uplift and inversion in the Upper Tertiary [2, 29]. These three phases of uplift stripped off significant part of the Permo-Triassic sandstones. The Permo-Triassic sandstones were deposited in alluvial fan, meandering river, playa and aeolian depositional environments [10]. The Permo-Triassic sandstones attain a thickness of 3000 meter at the basin center (depocenter) in the eastern part of the basin, while they are not more than 500 meter thick in the basin margin [10].

Mineralization in the Permo-Triassic sandstones, Ulster Basin, UK

In the Permo-Triassic sandstones, the precipitation of authigenic minerals and mineral transformation were controlled by temperature, geothermal gradient, burial depth and initial mineralogical composition, pore water types and circulation of the pore water. The Permo-Triassic sandstones experienced multiple phases of dissolution, replacement, precipitation and recrystallization, and thus have had a complex diagenetic history. The most common pore-filling minerals away from the volcanic intrusions in the eodiagenetic, mesodiagenetic and telodiagenetic regimes are: (1) concretionary carbonate and anhydrite, (2) grain coating illite-smectite and/or hematite, (3) pore-filling illite-smectite, (4) feldspar overgrowths (K-feldspar and albite), (5) quartz overgrowths, (6) poikilotopic calcite, dolomite and anhydrite, (7) kaolinite, and (8) hematite cement [10].

Era	Period	Formation	Lithology	Thickness (m)	Tectonic phase	Major litho-facies descriptive features			
CENOZOIC	Quaternary	Quaternary superficial deposits				Marine alluvium, peat, brown sand, river deposit, estuarine clay and glacial deposits			
	Tertiary	Upper Oligocene	Lough Neagh Group		0-769	Post basaltic movement	Siliciclastic (conglomerate, sideritic clay, flint, chert, sand, dark clay) and lignite		
		Paleocene-Miocene	U. Basalt Inter-basaltic horizon L. Basalt		0-1000	Sea floor spreading	Flood Basalt Upper Basalt: olivine basalt with minor trachyte and rhyolite Interbasaltic bed: conglomerate, flint, marl, lignite and ash beds L. Basalt: Alkaline olivine basalt with minor trachyte and rhyolite		
	MESOZOIC	Cretaceous	Upper	Ulster white Limestone		0-150	HERCYNIAN	Limestone (chalk) and hard ground	
Lower			Hibernian Sandstone		0-15	Green sandstone, grey marl, fossiliferous glauconitic sandstone			
Jurassic		Middle	Lias Mudstone		0-250	Post		Mudstone, fossiliferous argillaceous limestone	
		Lower	Rhaetic Mudstone		0-22	Post		Fossiliferous mudstone and shale	
Triassic		Upper	Mercia Mudstone Group		0-976	HERCYNIAN		Alternating sequences of argillaceous material (mudstone), arenaceous (sandstone) and evaporite (salt)	
		Middle	Sherwood Sandstone Group		0-857			Syn	Reddish brown sandstone with thin beds of mudstone and siltstone intercalation. Shaly at the top
		Lower							Mudstone and evaporite (salt)
Permian		Upper	Parmian Marl Magnesian Limestone		0-7 0-23	HERCYNIAN		Limestone	
		Lower	Permian Sandstone		0-2000			Early	Reddish brown sandstone with mudstone and shale. The upper and the lower parts are separated by 1500 m thick volcanic rocks
PALEOZOIC		Carboniferous	Upper	Westphalian Coal Measure		0-180		CALEDONIAN	Mudstone, shale, sandstone, with 8 coal seams (9.7 m thick)
	Namurian Rossmore Sandstone				0-609	Post	Mudstone, sandstone, with thin beds of conglomerate, and shale intercalation		
	Lower		Dinantian U. clastic Visian limestone, mudstone and sst Tournaisian lower clastics		0-180	Post	Upper clastic: sandstone and mudst.		
				0-2080	Post	Middle part: Alternating mudstone sandstone and limestone			
	Devonian	Upper	Old Red Sandstone		0-1676	Syn	Lower part: sandstone and basal conglomerate		
		Middle					Reddish brown sandstone (greywacke) and basal conglomerate		
	Silurian	Upper	Ordovician-Silurian meta-sediment and meta-volcanics		0-91	Pre-Early	Mudstone, greywackes, limestone, Meta-volcanics and meta-sediments		
		Lower					Mudstone, greywackes, limestone, meta-sediment and meta-volcanics		
	Ordovician	Upper			0-6553	Pre-Early			
	Precambrian		basment complex			Pangean Orogeny	Lewisian, Moirain, and Dalradian assemblages		

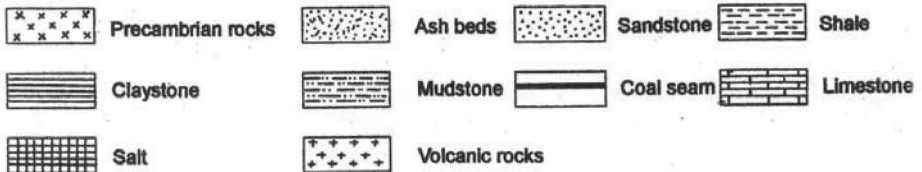


Figure 2. Chrono and lithostratigraphic and tectonic evolution of the Ulster Basin.

The sandstone beds in the vicinity of the volcanic intrusions contain authigenic minerals, actinolite, illite, laumontite and chlorite as cementations in addition to the many of the above mentioned minerals. Hematite cementation is absent near the volcanic intrusions. Early-stage diagenetic minerals (quartz overgrowths and feldspar overgrowths) were not affected by late-stage hydrothermal and heat-flow from the volcanic intrusions. Microcrystalline mosaic feldspar and quartz cements were not recorded near the volcanic intrusions in the Ulster Basin. The general relative sequence of the authigenic minerals is given in Figure 3.

Diagenetic sequence	Eodiagenetic	Mesodiagenetic	Telodiagenetic
Mechanical infiltrated clay	■		
Calcite cementation	■	■	
Evaporite cementation	■	■	
Dolomite cementation	■	■	
Mechanical compaction	■	■	
Grain dissolution	■	■	
Illite-smectite precipitation	■	■	
Hematite precipitation	■		■
Feldspar overgrowths	■	■	
Quartz overgrowths	■	■	■
Pressure dissolution		■	
Actinolite		■	
Chlorite		■	
Kaolinite		■	■
Cement dissolution			
Hydrocarbon migration		■	
Porosity gain			
Porosity loss			

Figure 3. Generalized mineral sequences of the Permo-Triassic sandstones.

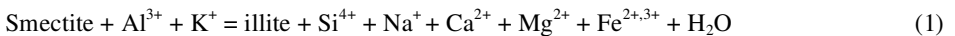
Cement types near the volcanic intrusions

Actinolite ($Ca_2(MgFe)_5(Si_4O_{11})_2(OH)_2$) cementation. Tertiary volcanic sills and dikes intruded the Permo-Triassic sandstones. Actinolite is one of the cement types in the studied samples. Actinolite mineralization took place only around the volcanic intrusions. This cement is widely distributed at Scrabo Quarry, and minor amounts are encountered in borehole BH-4B in the Lagan Valley. Thin fibrous rod-shaped and shard-like (sheaves) cement is identified by thin section and SEM studies (Figure 4a and c). It is associated with illite-smectite, authigenic quartz, K-feldspar and albite crystals (Figure 4a and c). Microprobe analyses revealed the presence of silicon, magnesium and iron oxides in the phase. Minor amounts calcium was also identified in the microprobe analyses. The presence of actinolite at the abandoned Scrabo Quarry and borehole BH-4B might be related to volcanic and hydrothermal effects [24, 10].

Transformation of smectite into illite [$K_{1-1.5}Al_4(Si_{7-6.5}Al_{1-1.5}O_{20})(OH)_4$] and *chlorite* ($(Mg,Fe)_3Al(AlSi_3)O_{10}$). The late-stage smectite precipitated as intergranular pore-filling cement. The dissolution of detrital feldspars and ferromagnesian minerals was the main source of ions for the authigenesis of smectite and illite-smectite. Pore-filling illite-smectite forms pore bridges between the grains, with a cellular or boxwork structure 2 to 15 μm thick. Illite-smectite is the most abundant intergranular pore-filling clay mineral in the studied samples. However, near the volcanic intrusions illite-smectite and smectite changed into illite and chlorite due to high temperature and hydrothermal activities. Fibrous illite projections are noted on box-work smectite near the volcanic intrusions (Figure 4c). Illite is characterized by hairy terminations, whereas smectite has a platy-hairy termination with cellular and boxwork texture. The abundance of illite near the volcanic intrusions reflects the transformation of smectite into illite. Illitization of smectite might have been favoured by potassium-rich alkaline pore water. Illite can also be precipitated from pore waters supersaturated with potassium, aluminium and silicon ions [cf. 30].

Chlorite is also identified by SEM studies, in the samples that were taken near the volcanic intrusions. Chlorite is more abundant in the Cultra and Tyrone samples. Chlorite is found in the form of individual plates and cabbage head-like morphotypes (Figure 4d). Most chlorite is associated with illite-smectite (Figure 4d).

The crystallization of smectite to illite liberated ions of silicon, calcium, magnesium and iron [31]. The late-stage intergranular pore-filling chlorite directly precipitated from silicon, aluminium, magnesium and iron-rich pore water, possibly favoured by transformation of smectite to illite due to high heat-flow. Magnesium and iron ions released from the volcanic activity and hydrothermal effects might have instigated precipitation of chlorite in the diagenetic environment. Microprobe analysis revealed the presence of potassium, magnesium, calcium, silicon, aluminium and iron, indicating that illite-smectite and chlorite could favourably be precipitated from the pore waters saturated with these ions.



Quartz (SiO_2) *overgrowths*. In most cases, quartz overgrowths (Figure 4a) post-dated the feldspar overgrowths. The dissolution of ferromagnesian minerals, feldspar grains and pressure solution activity possibly provided the necessary silicon ions. Spot counting microprobe analysis confirmed the presence of minor amounts of aluminium (< 1%) in some of the authigenic quartz crystals. In some cases, quartz overgrowths and feldspar overgrowths co-precipitated, competing for silicon ions. The late-stage volcanic intrusions and hydrothermal activity have not affected quartz overgrowths and crystals to develop microcrystalline mosaic of quartz.

K-feldspar ($KAlSi_3O_8$), albite ($NaAlSi_3O_8$) and laumontite ($CaAl_2Si_4O_{12} \cdot 4H_2O$) cementation. Near the volcanic intrusions the precipitation of *K*-feldspar, albite and laumontite were common. SEM and microprobe analysis confirmed the presence of both *K*-feldspar and albite overgrowths (Figure 4c), and laumontite (Figure 4b) in the studied samples. Incipient feldspar overgrowths might have commenced in the eodiagenetic regime. The dissolution of ferromagnesian (mafic) minerals and feldspar grains introduced the necessary ions for the precipitation of authigenic *K*-feldspar, albite and laumontite. The albite overgrowths are discontinuous upon the detrital *K*-feldspar grains, whereas the *K*-feldspar overgrowths are continuous upon the *K*-feldspar grains.

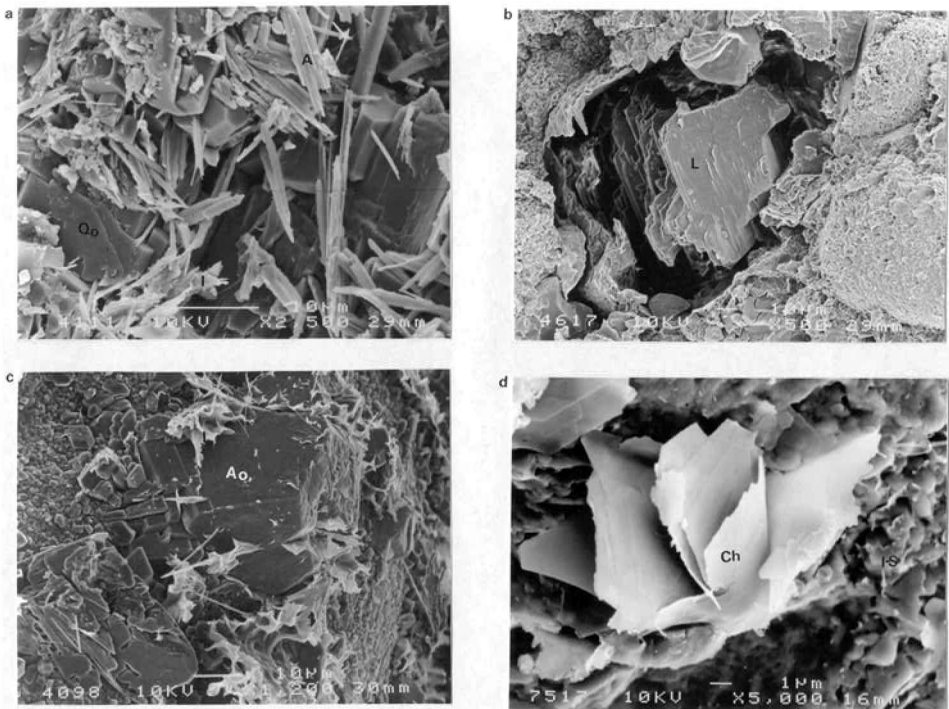


Figure 4. (a) SEM photomicrograph showing quartz crystal (Qo), Actinolite (A) and illite (I). Triassic sandstone, outcrop sample, Scrabo Quarry, Ulster Basin (scale bar 10 microns). (b) SEM photomicrograph showing laumontite (L) Triassic sandstone, outcrop sample, Cultra section, Ulster Basin (scale bar 10 microns). (c) SEM photomicrograph showing albite (Ao), illite (I) and actinolite (A), outcrop sample, Scrabo Quarry, Ulster Basin (scale bar 1 micron). (d) SEM photomicrograph showing well developed cabbage head chlorite (Ch) and illite-smectite (I-S), outcrop sample, Cultra section, Ulster Basin (scale bar 1 micron).

Mineral transformation from *K*-feldspar to albite is commonly observed near the intrusions. The zoned areas identified in the studied samples indicate that there was a partial replacement of *K*-feldspar by sodium-rich pore water. During deeper burial albitization of detrital *K*-feldspar took place favoured by sodium-rich alkaline pore waters that possibly resulted from transformation of smectite into illite [cf. 32]. Dissolution of plagioclase often results in precipitation of albite. Albite crystals are widely distributed in the abandoned Scrabo Quarry and

Cultra areas, which are known to have been volcanic dikes and sills. Laumontite is also documented in samples obtained from near the volcanic intrusions.

Hematite cementation. Away from the volcanic intrusions late-stage hematite precipitation took place in the secondary porosity. Gravity-driven oxidizing meteoric water might have provided the necessary ions to cause the precipitation of hematite. The presence of hematite is an indicator for an oxidizing environment. However, hematite cementation is absent near the volcanic intrusions, possibly due to bleaching away by hot fluids.

Background geology of the Hartford Basin

The Hartford Basin developed by crustal extension associated with the breaking up of Pangea and the opening of the Atlantic Ocean [17]. The basin was infilled with 4500-5000 meters thick clastic sediments including alluvial fans, playa red beds, lacustrine grey and black strata, and extrusive tholeiitic basalts [10, 12, 14]. The 2 km thick alluvial fan and fluvial red bed-dominated New Haven Arkose was deposited when the rate of sedimentation exceeded the rate of basin subsidence. The Shuttle Meadow and the East Berlin Formations were deposited when the subsidence rate increased to exceed the rate of sedimentation [10, 14]. The sedimentation was accompanied by volcanic activity in the Hartford Basin. The geological map and chrono-lithostratigraphic section of the Hartford Basin are shown in Figure 5 and 6 respectively.

Mineralization in the Triassic-Jurassic sandstones, Hartford Basin, USA

The most common paragenetic pore-filling minerals in the studied sandstone formations are: (1) mechanical infiltrated clay, (2) grain coating illite-smectite/hematite, (3) concretionary calcite and dolomite, (4) feldspar overgrowths, (5) quartz overgrowths, (6) carbonate cements (dolomite, ferroan dolomite, calcite, ferroan calcite and ankerite), (7) pore-filling kaolinite, illite-smectite and smectite-chlorite, (8) hematite, (9) pyrite and (10) apatite [10].

The following minerals are recorded near the volcanic intrusions: (1) microcrystalline mosaic albite and quartz, (2) transformation of K-feldspar into albite, (3) transformation of mechanically infiltrated smectite into authigenic clay minerals (illite and smectite), and (4) transformation authigenic illite-smectite and smectite into illite and chlorite. The diagenetic minerals sequence is shown in Figure 7 and 8.

Cement types near the volcanic intrusions

Mechanically infiltrated clay. Mechanically infiltrated clays dominated by smectite and illite-smectite are found widely distributed in the studied sandstone samples. SEM studies confirmed the presence of cutans around the detrital framework grains (Figure 9a). Mechanically infiltrated clay lies tangential to the grain surfaces, and settled out in contact with impermeable layers. In late-stage diagenesis, mechanically infiltrated clay near the volcanic dikes and sills was transformed to authigenic clay minerals. Authigenic clay began to grow first along the edge of the fragmented cutans, and totally covered them at the later stages. Adjacent to the basaltic dikes and sills the infiltrated clay is changed to authigenic clay minerals due to high heat-flow and magnesium and iron-rich hydrothermal fluids. This transformation is visible by gradual upturning and curling of edges of the smooth illite-smectite coating, and finally to fibrous illite and cabbage head-like chlorite. Rocks with abundant infiltrated clay have a restricted diagenetic evolution. In the Hartford Basin, quartz overgrowths, feldspar overgrowths, carbonate cements and porosity enhancement were retarded by the presence of abundant mechanically infiltrated clay.

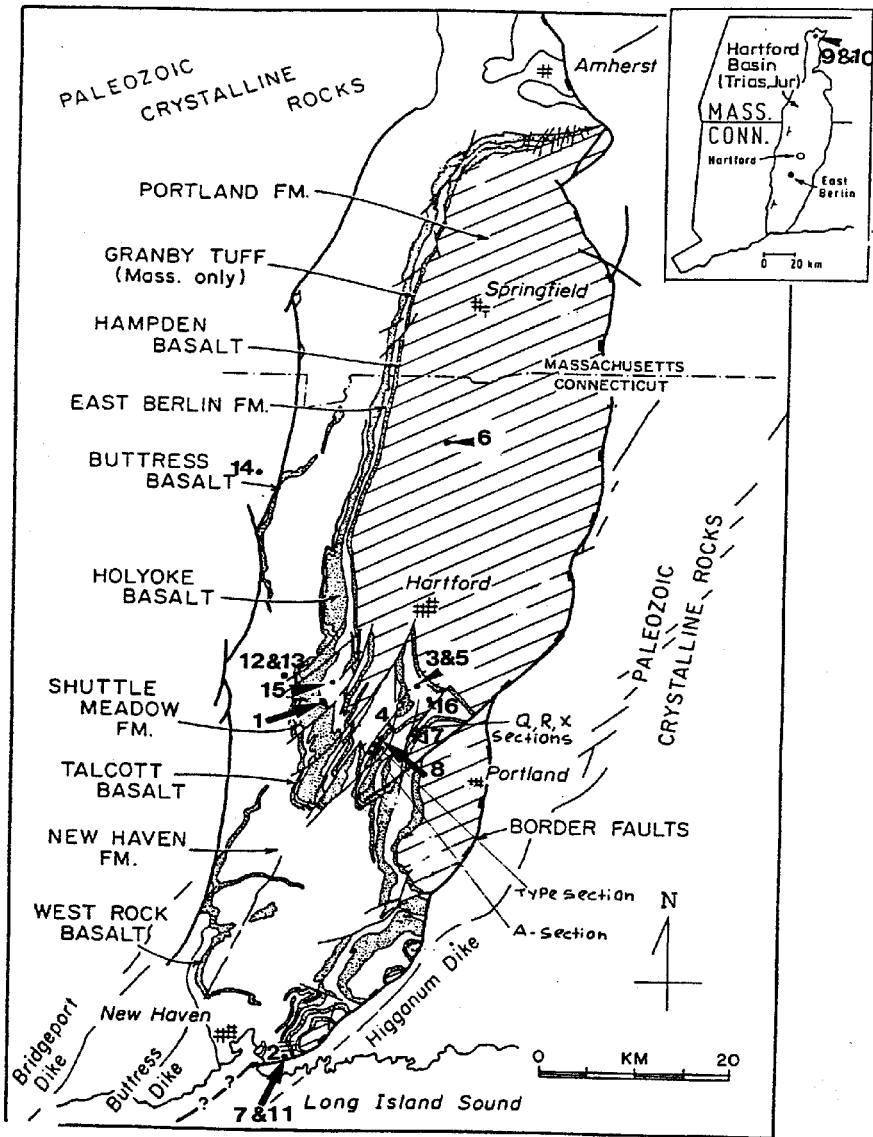


Figure 5. Geological map of the Hartford Basin and sample location of studied areas in the Hartford Basin.

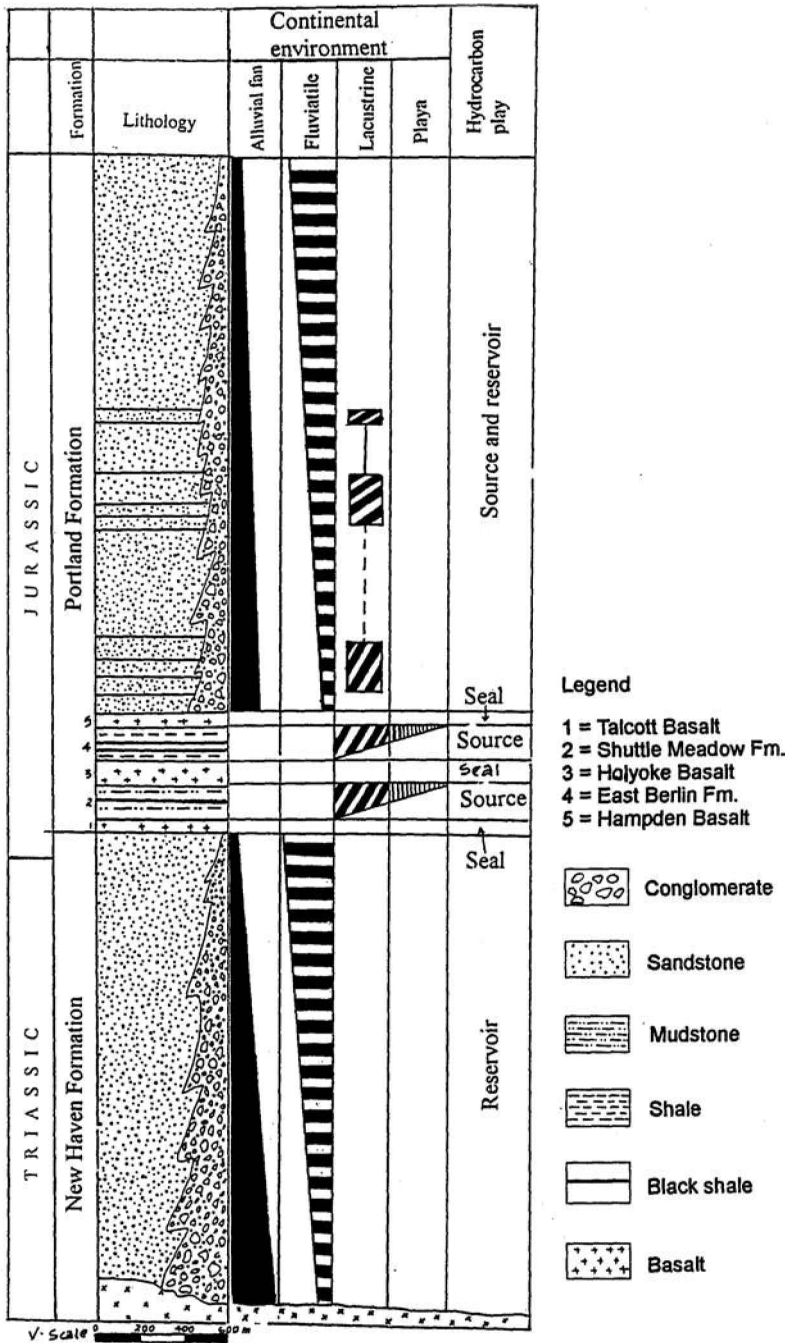
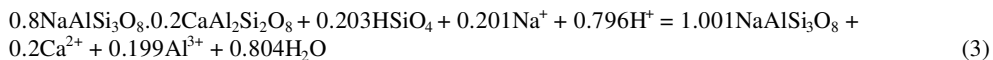
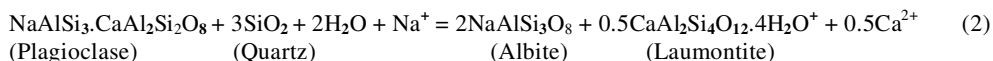


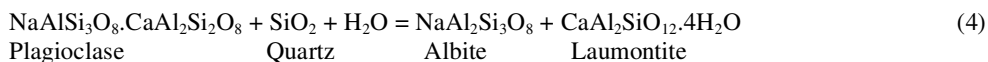
Figure 6. Chrono, litho-stratigraphic section and depositional environments and hydrocarbon plays of the Hartford Basin.

Albitization and laumontization. SEM and microprobe examination confirmed albite and laumontite cements around the basaltic dikes and sills. Partial albite overgrowths, crystals and complete albitization with euhedral rhombohedral faces were identified. Zoned areas are identified in the studied samples (Figure 9c), in which there is minor fluctuation in potassium and sodium concentration. The K-feldspar grains are optically discontinuous with the overgrowths. The core is K-feldspar whereas the overgrowth rims show an albite composition. Albitization occurred both as fracture filling and overgrowths on detrital K-feldspar. The albitization process is more sensitive to potassium removal than sodium supply [37]. The possible causes for albitization processes are considered to be the amount of grain surface in contact with the pore fluids, the degree of fracturing of grains, pore water composition and structural state [38]. Selective leaching of K-feldspar is related to illite transformation. The illitization of smectite takes place between 60-100° C [31], which also coincides with the zone of albitization. Albitization of K-feldspar occurs between 65-120° C at a depth range from 1400 to 4200 m [37].

Equant to lath-shaped laumontite were also identified samples near the volcanic intrusions by SEM and microprobe studies (Figure 9d). EDX and probe analyses showed the presence of calcium, aluminium and silicon ions. The presence of albite and laumontite is explained by the replacement of calcic plagioclase, which proceeds as an equal volume replacement reaction with sodium ions from solution [32].



Laumontization was initiated when calcium-bearing plagioclase was partly replaced by laumontite. For a given volume of plagioclase altered, an equal volume of albite-laumontite intergrowth plus addition of laumontite will be produced to replace quartz-filled pores [32]:



The transformation of smectite to illite has released considerable amounts of sodium ions as a precursor for albitization [24, 10, 21, 31, 36]. As the pore water became enriched in sodium ions from the conversion of smectite to illite and a continuous supply of sodium facilitated albitization of calcium-bearing plagioclase, which in turn released calcium ions necessary for the generation of laumontite in the Ulster Basin and Hartford Basin [cf. 39].

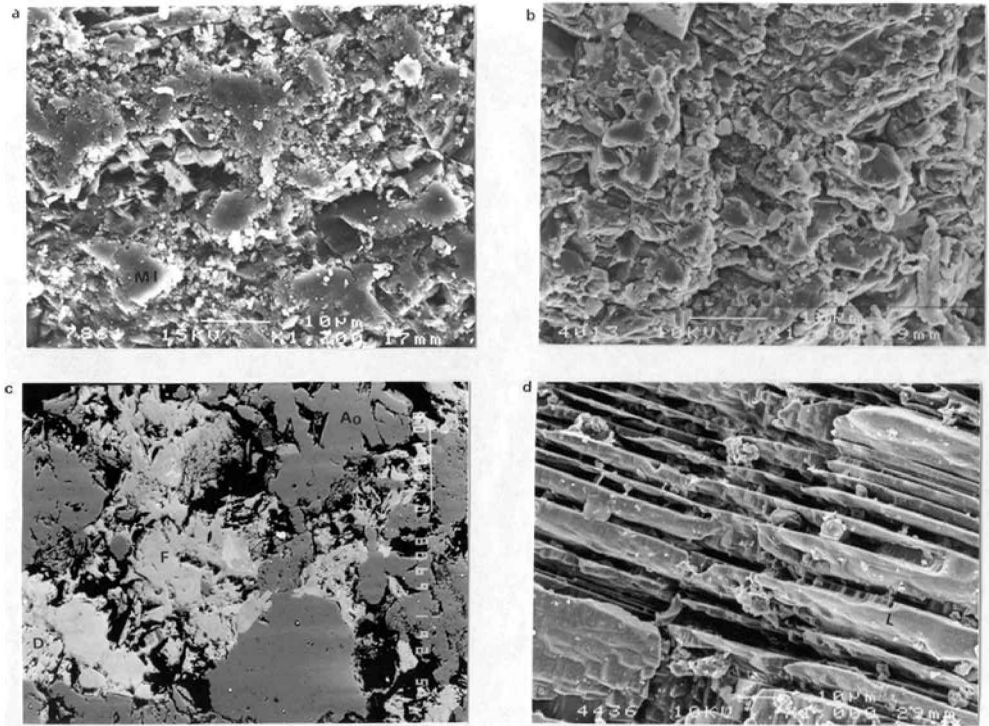


Figure 9. (a) SEM photomicrograph showing mechanically infiltrated clay (MI), X-12, outcrop cross-laminated siltstone, East Berlin Formation, Hartford Basin (scale bar 10 microns). (b) SEM photomicrograph showing microcrystalline mosaic quartz and albite, CB-01, outcrop sample, Cherry Brook, Hartford Basin (scale bar 10 microns). (c) SEM photomicrograph showing albitization (Ao) of K-feldspar (F) and dolomite, CTV-3, outcrop sample, New Britain, Hartford Basin (scale bar 10 microns). (d) SEM photomicrograph showing laumontite (L), CTV-10, 372-5 slip road, East Berlin Formation, Hartford Basin (scale bar 10 microns).

SUMMARY AND CONCLUSIONS

In the Hartford Basin, the volcanic intrusions took place simultaneously with the sedimentation of Triassic-Jurassic sandstones. The basaltic eruption and hydrothermal activity modified the texture of feldspar overgrowths and quartz overgrowths in the Hartford Basin. Elevated heat-flow and hydrothermal activity near the basaltic dikes and sills initiated the formation of microcrystalline mosaic albite and quartz rather than overgrowths. This feature is not common, and very localized near the basaltic dikes and sills. The abundance of albite and quartz overgrowths crystals increase at distances a few meters away from the volcanic intrusions. Simultaneous volcanic activity in the Hartford Basin modified the diagenetic sequences of the sandstones near the intrusions. Chlorite clumps/masses within the microcrystalline mosaic albite and quartz are also documented near the volcanic dikes and sills. Laumontite is also abundantly documented near the volcanic intrusions.

In the Hartford Basin, mechanically infiltrated clays (illite-smectite and smectite) changed into authigenic clay minerals near the intrusions. Authigenic illite-smectite and smectite are also

changed into illite and chlorite. Hematite is absent near the volcanic intrusions, and assumed to have been bleached away by hot fluids.

In the Ulster Basin, the Permo-Triassic sandstones were intruded by Tertiary volcanic intrusions (dikes and sills). Most of the authigenic mineralization pre-dated the Tertiary volcanic intrusions. Authigenesis of quartz and feldspar took place before the Tertiary volcanic activity. Quartz and feldspar overgrowths were not affected by the late-stage heat-flow and hydrothermal activity from the volcanic intrusions. Mineral transformations were exhibited near the volcanic intrusions. Transformation of K-feldspar into albite was well documented. Illite-smectite transformed into chlorite cementation. Late-stage fibrous illite, chlorite, albite, laumontite and actinolite cementation were also documented near the dikes and sills. The abundance of chlorite, illite, laumontite, albite and actinolite cements decreases away from the volcanic intrusions.

The type of minerals formed at the time of sandstone diagenesis affect the reservoir characteristics. In the studied sandstone formations, temperature, pore fluid chemistry, and fluid flow affect the reservoir characteristics. This study confirmed that heat-flow and hydrothermal activity from the volcanic dikes and sills modified the textural and mineralogy of sandstones. The change of smectite to illite and chlorite, formation of albite, laumontite, feldspar mosaic, quartz mosaic and actinolite modified the reservoir characteristics. Illite reduces permeability considerably by blocking pore throat. Studies shows illite-cemented sandstone does not exceed 1 mD. Porosity and permeability is also reduced by shard-like sheaves of actinolite. Pore-bridging smectite and chlorite have the worst effect in destroying the porosity and permeability. The albite and laumontite precipitated in the secondary pore spaces reduced porosity and permeability of the studied sandstone samples near the intrusions. Laumontite has the worst effect in destroying the reservoir characteristics. Samples that have been collected away from the intrusions have porosity value ranging from 5.4 to 27.4% and permeability up to 1350 mD. However, samples that were collected 5 meters both sides of the intrusions, the porosity range from 0-1.2% and permeability of less than 1 mD. From this study, it is possible to conclude that large volcanic intrusions that are found within the sandstone bodies have significant impact in the reservoir characteristics in oil exploration.

ACKNOWLEDGEMENTS

The constructive comments of Dr. J. Parnell on the draft manuscript are gratefully acknowledged. I am indebted to Dr. E. Gierlowski-Kordesch, Dr. A. Ruffel, Mr. A. Assefa, T. Ketsela, and the Bulletin referees for their constructive and valuable reviews of the manuscript. Most of the work was carried out at the School of Geosciences, the Geochemical Laboratory and the Electron Microscopy Unit, the Queen's University of Belfast. The author acknowledges the Ministry of Mines and Energy, Ethiopia and the School of Geosciences, the Queen's University of Belfast for financial support.

REFERENCES

1. Naylor, D. *Basin on the Atlantic Seaboard: Petroleum Geology, Sedimentology, and Basin Evolution*, Parnell, J. (Ed.); Geol. Soc. Lond. Spec. Publ., Vol. 62, Geological Society of London: London; **1992**, pp 255-275.
2. Wilson, H.E. *Regional Geology of Northern Ireland*, N. Ireland Geological Survey: Belfast, UK; **1986**.
3. McCann, N. *Ir. J. Ear. Sci.* **1988**, 9, 171.
4. McCann, N. *Ir. J. Ear. Sci.* **1990**, 10, 71.
5. McCann, N. *Ir. J. Ear. Sci.* **1991**, 11, 53.

6. McCaffery, R.J.; McCann, N. *Basins on the Atlantic Seaboard: Petroleum Geology, Sedimentology and Basin Evolution*, Parnell, J. (Ed.); Geol. Soc. Lond. Spec. Publ., Vol. 62, Geological Society of London: London; **1992**, pp 277-290.
7. Parnell, J. *J. Petrol. Geol.* **1991**, 14, 65.
8. Parnell, J. *J. Petrol. Geol.* **1991**, 14, 143.
9. Parnell, J. *J. Petrol. Geol.* **1992**, 15, 51.
10. Ahmed, W. *Ph.D. Thesis*, The Queen's University of Belfast, UK, **1997**.
11. Demicco, R.V.; Gierlowski-Kordesch, E. *Sedimen.* **1986**, 33, 107.
12. Gierlowski-Kordesch, E.; Huber, P. *State Geological and Natural History Survey of Connecticut*, **1995**; Guide Book No-7: B1.
13. Lorenz, J.C. *Triassic-Jurassic Rift-Basin Sedimentology: History and Methods*, Van Nostrand Reinhold: New York; **1988**.
14. Hubert, J.F.; Feshbach-Meriny, P.C.; Smith, M.A. *AAPG Bull.* **1992**, 76, 1710.
15. Fairbridge, R.W. *Geolo. Minjnb.* **1979**, 58, 273.
16. Manning, A.H.; de Boer, J.Z. *Geol.* **1989**, 17, 1016.
17. Manspeizer, W. *Triassic-Jurassic Rifting: Continental Break-up and the Origin of the Atlantic Ocean and Passive Margin*, Part A., Manspeizer, W. (Ed.); Elsevier: Amsterdam; **1988**; pp 41-80.
18. Schlische, R.W. *Tect.* **1993**, 12, 1026.
19. Wenk, W. *J. North. Geol.* **1990**, 6, 202.
20. Merino, E. *J. Sed. Petrol.* **1975**, 45, 320.
21. Van de Kamp, D.C.; Leake, B.E. *Chem. Geol.* **1996**, 133, 89.
22. Bjorlykke, K. *Diagenesis I, Development in Sedimentology*, Chilingarian, G.V.; Wolf, K.H. (Eds.); Elsevier: Amsterdam; **1988**, pp 555-588.
23. Elzea, J.M. *Northeast. Sec. Geol. Soc. Am., Abstract Volume* **1987**; p 12.
24. Helmold, K.P.; Van de Kamp, P.C. *Clastic Diagenesis*, McDonald, D.A.; Surdum, R.C. (Eds.); AAPG Mem. 37, American Association of Petroleum Geologists: Oklahoma, USA; **1984**; pp 239-276.
25. Bjorlykke, K. *Sediment Diagenesis*, Vol. 115, Parker, A.; Sellwood, B.W. (Eds.); D. Reidel Publishing Company: Dordrech, Holland; **1983**; pp 169-213.
26. School, P.A. *A Colour Illustrated to Constituents, Texture, Cement and Porosities of Sandstones and Associated Rocks*, AAPG Mem. 28, American Association of Petroleum Geologists: Oklahoma, USA; **1979**.
27. Welton, J.E. *SEM Petrology Atlas (Method in Exploration Series)*, American Association of Petroleum Geologist: Oklahoma, USA; **1984**; p 237.
28. Pye, K.; Krinsley, O.H. *J. Sed. Petrol.* **1984**, 54, 877.
29. Coward, M.P. *Permian and Triassic Rifting in Northwestern Europe*, Vol. 91, Bodly, S.A.R. (Ed.); Geol. Soc. Lond. Spec. Publ., Geological Society of London: London; **1995**; pp 7-39.
30. Macchi, L. *Geol. J.* **1987**, 22, 333.
31. Hower, J.; Eslinger, E.V.; Hower, M.E.; Perry, E.A. *Geol. Soc. Am. Bull.* **1976**, 87, 725.
32. Boles, J.R. *Am. J. Sc.* **1982**, 282, 165.
33. Ali, A.D.; Turner, P. *J. Sed. Petrol.* **1982**, 52, 187.
34. Heald, M.T. *J. Geol.* **1956**, 64, 17.
35. Waught, B. *J. Geol. Soc. London* **1978**, 135, 51.
36. Worden, R.H.; Rushton, J.C. *J. Sed. Petrol.* **1992**, 62, 779.
37. Aagaard, P.; Egeberg, P.K.; Saigal, G.C.; Morad, S.; Bjorlykke, K. *J. Sed. Petrol.* **1990**, 60, 575.
38. Ramseyer, K.; Boles, J.M.; Lichtner, P.C. *J. Sed. Petrol.* **1992**, 62, 349.
39. Boles, J.R.; Coombs, D.S. *Am. J. Sci.* **1977**, 277, 982.